



# Insight in the interaction mechanisms between functionalized CNTs and BTX vapors in gas sensors: Are the functional peripheral groups the key for selectivity?

Amadou Ndiaye, A. Pauly, J. Brunet, C. Varenne

## ► To cite this version:

Amadou Ndiaye, A. Pauly, J. Brunet, C. Varenne. Insight in the interaction mechanisms between functionalized CNTs and BTX vapors in gas sensors: Are the functional peripheral groups the key for selectivity?. Sensors and Actuators B: Chemical, 2019, 298, pp.126768. 10.1016/j.snb.2019.126768 . hal-02372035

**HAL Id: hal-02372035**

**<https://uca.hal.science/hal-02372035>**

Submitted on 25 Oct 2021

**HAL** is a multi-disciplinary open access archive for the deposit and dissemination of scientific research documents, whether they are published or not. The documents may come from teaching and research institutions in France or abroad, or from public or private research centers.

L'archive ouverte pluridisciplinaire **HAL**, est destinée au dépôt et à la diffusion de documents scientifiques de niveau recherche, publiés ou non, émanant des établissements d'enseignement et de recherche français ou étrangers, des laboratoires publics ou privés.



Distributed under a Creative Commons Attribution - NonCommercial 4.0 International License

# Insight in the interaction mechanisms between functionalized CNTs and BTX vapors in gas sensors: are the functional peripheral groups the key for selectivity?

A. Pauly<sup>1</sup>, J. Brunet<sup>1</sup>, C. Varenne<sup>1</sup>, A. L. Ndiaye<sup>1\*</sup>

<sup>(1)</sup> Université Clermont Auvergne, CNRS, Sigma Clermont, Institut Pascal, F-63000

Clermont-Ferrand, France

Email: [amadou.ndiaye@uca.fr](mailto:amadou.ndiaye@uca.fr)

## Abstract:

Herein we focus on gas sensor responses of both organic macrocycles (MCs) and carbon nanotubes (CNTs) functionalized with MCs (CNTs/MCs) to understand the interaction mechanisms of these materials exposed to aromatics volatile organic compounds (VOCs) such as benzene, toluene and xylene (BTX). The MCs-functionalized CNTs are prepared by non-covalent functionalization using phthalocyanines and porphyrins derivatives. We focus our analysis on the peripheral groups of both the MCs (tert-butyl, phenyl, ethyl) and BTX (methyl) by means of the analyses of both the desorption kinetics and surface interactions. A cross-analysis between the physisorption phenomena and kinetics of the responses is found to be relevant for understanding the interactions. The analysis of the sensing performances at room temperature (25 °C) for the MCs-based QCM sensors revealed that the nature of the peripheral moieties (aryl or alkyl of the MCs alone) dictates the kinetics and the desorption profile whatever the VOC. The similar analysis conducted on the sensing performances of the CNTs/MCs-based QCM sensors shows that, methyl groups of the BTX are the dominant parameter that modulate the response profile whatever the hybrid materials. A focus on dispersion interactions and desorption kinetics allows to evidence that the interaction between

the VOCs and MCs or CNTs/MCs is reinforced or weakened depending on the peripheral moieties from the MCs or BTX. From this study, it is clearer that substituents of the VOCs are more important for kinetics of desorption than the functional groups of the CNTs/MCs.

**Keywords: Functionalization, Macrocycle, BTX, Carbon nanotubes, Dispersion interaction, Sensors**

## **1. Introduction:**

Carbon nanotubes and their functionalized derivatives have, in the last years, contributed a lot in the research on gas sensors [1-2]. Reasons for such a devotion are clearly attributed to their higher surface area but also to their versatile surface chemistry which enables functionalization in a covalent or non-covalent way [3]. For their use as sensors, their unique electronic and optical properties [1] as well as their surface sensitivity are important. And this allows them to be useful as chemi-resistors [4], mass sensors [2] or optical sensors. At the beginning, the use of CNTs as potential sensing materials suffered from their lack of solubility and their natural bundling configuration. In terms of processing these problems represent some hurdles for the an easy and low cost processing. However, progress in chemical functionalization has proven to be strategically helpful to partially solve the lack of solubility while simultaneously affording new properties. Besides this utility, the chemical functionalization is also intended to bring specific function to the CNTs surfaces and provide more reactivity towards targeted gases [5]. It is well known that incorporating defects, which can be consider, to a smaller extent, as a surface functionalization, is beneficial for enhancing the surface reactivity of pristine CNTs toward gases [6]. The use of surface functionalization to control and monitor surface reactivity of CNTs through attachment of functional moieties has been therefore developed for application in the field of gas sensors [2].

Many researches on nanocarbon based gas sensors [7-8] have been oriented on the functionalization of CNTs to target aromatics VOCs such as BTX. These aromatic

compounds are species whose levels in both indoors and outdoors [9-10] have increased considerably.

The first motivation behind the use of the functionalization to make the CNTs highly sensitive to BTX came from the propensity of the CNTs surface, essentially made of benzene rings (hexagonal unit), to interact with the aromatics VOCs via  $\pi$ - $\pi$  interactions as in the benzene dimer [11]. For the same reasons, rich  $\pi$ -electrons molecules are promoted to assess functionalization in a non covalent way. Phthalocyanines (Pc) and porphyrins (Por) derivatives as  $\pi$ -electrons systems are good candidate to fulfil the functionalization requirement via covalent or non covalent bonding [12-14]. Furthermore they exhibited a great interest for the detection of VOCs [15-23]. In the last years, we have focussed on the functionalization of CNTs by phthalocyanines and porphyrins derivatives aimed to incorporate specific functional groups to target BTX vapors. We previously reported the case study of toluene [24], and later on benzene and xylene [25]. Our objective was to get insight into the mechanism and evaluate how functional groups on both the MCs and VOCs affect the surface reactivity of CNTs/MCs.

This paper is the final piece of the puzzle which aimed to formalize the mechanisms of interaction taking place between the functionalized CNTs and the aromatic BTX. Thus, the sensing behaviour of three macrocycles (phthalocyanines and porphyrins denoted CuPctBu, OEPH<sub>2</sub>, TPPH<sub>2</sub>) as well as their functionalized CNTs parts (CNTs/CuPctBu, CNTs/OEPH<sub>2</sub>, CNTs/TPPH<sub>2</sub>) will be analyzed through their interaction kinetics and adsorption/desorption profile. Combined analysis of the sensitivity and kinetics will give rise to correlations that will guide us to propose a schematic representation to elucidate the sensing mechanisms. Finally we will take the advantage of using the combination of the transduction modes and the sensor performances, to understand the synergy that governs gas/material interactions in terms of electronic conductivity and surface exchange. This later will be analyzed as an

interplay between  $\pi$ - $\pi$ , alkyl-alkyl and  $\pi$ -alkyl interactions (van der Waals interactions) as well. A discussion aimed to orientate the selectivity issue is proposed at the end.

## **2. Experimental**

### **2.1. Chemicals and Solvents**

Anhydrous chloroform (purity grade >99%) was obtained from Aldrich and used without further purification procedure. Single walled carbon nanotubes (raw-SWNTs) obtained from a chemical vapor deposition (CVD) process were purchased from Helix Material Solutions and were used as received (purity grade >90%). Copper(II) 2,9,16,23-tetra-tert-butyl-29H,31H-phthalocyanine (purity 97%, denoted CuPctBu), 2,3,7,8,12,13,17,18-octaethyl-21H,23H-porphine (purity 97%, denoted OEPH<sub>2</sub>), and 5,10,15,20-tetraphenyl-21H,23H-porphine (purity 97%, denoted TPPH<sub>2</sub>), were obtained from Aldrich and used without further purification.

### **2.2. Materials preparation and characterization**

Unless otherwise stated all experiments were conducted at room temperature (25°C). The experimental parts will not be fully developed, readers are invited to see article [24] for more details. The preparation and synthesis of the hybrid materials follow a procedure which has been described earlier [24]. The CNTs are dispersed into a solution containing the macrocycles. After sonication, a discoloration of the macrocycle solution occurs, demonstrating the adsorption of macrocycles on the CNTs walls. Through the measurement of the absorption difference using UV-Vis spectroscopy, it is possible to confirm the functionalization. As an example, 1 mg of CNTs were immersed in a chloroform solution of 0.005 mM OEPH<sub>2</sub> and then the resulting mixture was sonicated for 15 min. The residual material, collected after sonication and centrifugation, is then washed several times with chloroform and dried. In the sensor preparation procedure, the materials were thoroughly re-

dispersed in chloroform prior to deposition. The same procedure apply for functionalization of CNTs with TPPH<sub>2</sub> or CuPctBu.

### **2.3. Sensor devices preparation**

For the realization of resistive sensors, interdigitated electrodes (IDEs) made of platinum screen printed on alumina substrate, with interelectrode distance of 125  $\mu\text{m}$ , were used. The functionalized CNTs were dispersed in chloroform and drop-casted on the IDEs. The coating were then dried at 80 °C during 1h and I-V characterization performed at room temperature (25 °C). The electrical characteristics (I-V curves) were obtained from Keithley 2636 System Source Meter which is controlled by a Labview program.

For the realization of the mass sensors we used commercially available 5 MHz AT-cut QCM substrates from INFICON with the following characteristics: sensitivity factor  $C_f$  of 0.056 Hz/ng/cm<sup>2</sup>, area of 1.37 cm<sup>2</sup>, and Cr/Au electrodes on both sides. The functionalized materials were dispersed in chloroform and drop-casted on one side of the QCM substrate and dry at 80 °C. The mass sensors are further stored at room temperature (25 °C) before exposure experiments. The frequency variations were measured by a frequency counter Agilent 5313A.

### **2.4. Gas sensing experiments**

For gas exposure experiments, a dilution bench consisting of pollutant source, the chamber and a computer assisted data acquisition and collection program monitored through a Labview software form the test bench. The gas source was diluted with dry air (corresponding to relative humidity of around 3 %) to obtain the desired concentration range. For relative humidity experiments, a humidity control system is adapted to the test bench to provide relative humidity percentage between 10% and 90%. For the resistive sensors, the IDEs coated with functionalized CNTs were used as sensors and the resistance variations measured by a Digital Multimeter (Keithley 2700). For the mass sensors, the functionalized

materials were deposited onto commercially available 5 MHz AT-cut QCM substrates from INFICON with the following characteristics: sensitivity factor Cf of 0.056 Hz/ng/cm<sup>2</sup>, area of 1.37 cm<sup>2</sup> with polished Cr/Au electrodes on both sides. The frequency variations were measured by a frequency counter Agilent 5313A.

Unless otherwise specified in the article, the sensor response is defined as a signal variation of a measured parameter (frequency or resistance) under air zero (purified air) and under gas exposure. For the mass transduction, we defined the QCM responses as the frequency variation ( $\Delta F$ ) normalized to the amount of deposited material given in nanogram (ng). ( $\Delta F$ ) corresponds to the difference between the frequency under air zero ( $F_0$ ) and the frequency under gas exposure ( $F_{\text{gas}}$ ) i.e.  $\Delta F = F_0 - F_{\text{gas}}$  of the sensors. Therefore the QCM responses are given in herz per nanogram (Hz/ng). For the resistive transduction, the resistive sensors responses are given as resistance variation ( $\Delta R$ ) representing the difference between resistance under air zero ( $R_0$ ) and resistance under VOCs vapors ( $R_{\text{Gas}}$ ) i.e. ( $\Delta R = R_{\text{Gas}} - R_0$ ). All experiments were conducted at room temperature (25°C) in dry air environment (1-3% relative humidity). Response time ( $\tau_{\text{resp}}$ ) is defined as the time needed to reach 90% of the maximum response amplitude while recovery time ( $\tau_{\text{rec}}$ ) is defined as the time needed to recover 90% of background signal. Sensitivity of the sensors is defined as the response (Hz/ng for the mass sensors) per unit concentration (ppm) and is given in Hz/ng/ppm for the mass sensors.

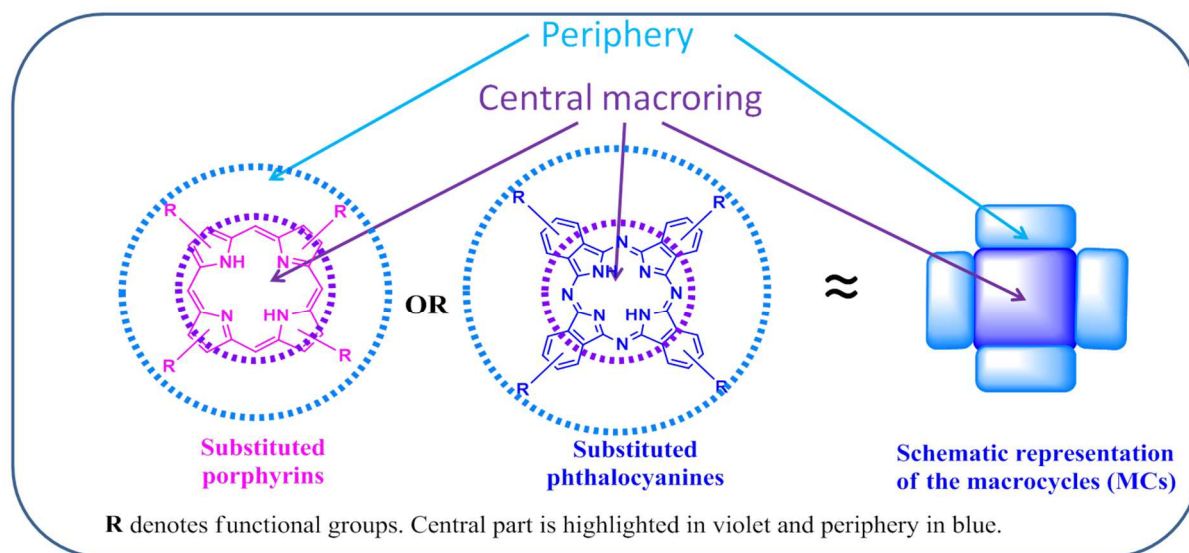
### **3. Results and Discussion**

We will firstly discussed the responses of the macrocycles (MCs) before those of the hybrid materials (CNTs/MCs) toward BTX.

#### **3.1. Sensor performances of the free MCs exposed to BTX: what the MCs reactivity can afford for understanding the reactivity with VOCs.**

### 3.1.1. VOCs, MCs and their potential interactions

As the discussion will be oriented on the functional groups (substituents), Scheme 1 gives a statement on the functional groups and their potential interactions. Table 1 defines the structure of the VOCs in relation with the potential interactions that can take place.



Macrocycles	CuPctBu	OEPH <sub>2</sub>	TPPH <sub>2</sub>
Nature of the central part	Aromatic	Aromatic	Aromatic
Functional groups of the periphery	Tert-butyl (4)	Ethyl (8)	Phenyl (4)
Potentially existing peripheral alkyl interactions	✓	✓	-
Potentially existing peripheral $\pi$ interactions	✓	-	✓

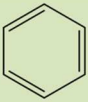
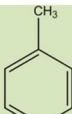
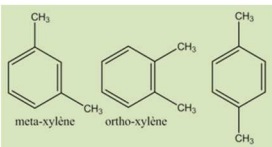
**Scheme 1: Schematic presentation of the different macrocycles (MCs) (upper panel) and the potentially existing type of interactions induced by the peripheral groups (lower panel).**

The macrocycles can be viewed as a molecular structure made of two entities: i) a central part essentially localized around a macrocyclic ring delimited by meso-nitrogens which concentrate the aromatic center, and ii) the periphery composed of different peripheral groups surrounding the central part as given in the upper panel of Scheme 1. Here we consider the global aromaticity taking into account the macrocyclic conjugation more than the local aromaticity which involves the pyrrolic five membered ring. Based on such a representation, both the



alkyl interactions and  $\pi$ - $\pi$  interactions (van der Waals) can be envisaged as potentially existing interactions from the peripheral groups.

**Table 1: Studied VOCs and their potential type of interactions with aromatic center or alkyl groups.**

VOCs	 Benzene	 Toluene	 meta-xylene, ortho-xylene, para-xylene
Nature of the central part	Aromatic	Aromatic	Aromatic
Functional groups of the periphery	-	-Methyl (1)	-Methyl (2)
Potentially existing peripheral alkyl interactions	-	✓	✓
Potentially existing peripheral $\pi$ interactions	✓	✓	✓

If we make the same analysis on the VOCs, we can assume that peripheral alkyl groups situated around the benzene ring will potentially be subject to alkyl interactions while the aromatic centers themselves will potentially be subject to  $\pi$ -interactions. As an example, benzene has no peripheral alkyl groups and is therefore only concerned with  $\pi$ -interactions. For the same reasons toluene and xylene with their methyl groups, will potentially be subject to both type of interactions.

### 3.1.2. Sensor performances of the macrocycles toward BTX exposures

If the macrocycles CuPctBu, OEPH<sub>2</sub> or TPPH<sub>2</sub> are exposed to xylene a general decrease in frequency is observed as in Fig. 1. The same behavior is also noticed for benzene (Fig. S1; see supporting information). This decrease is a consequence of vapors adsorption onto the surface of the sensing materials as predicted by the sauerbrey equation [26]. A quick analysis of the frequency shift as represented in Fig. 1, allows to see that frequency variation at ca. 500ppm xylene concentration is around 13 Hz for the OEPH<sub>2</sub>, 19 Hz for the CuPctBu and 44

Hz for the TTPH<sub>2</sub>. Fig. 1 also shows that recovery of the frequency signal is faster for the OEPH<sub>2</sub>, but details on the kinetics will be given later in this section.

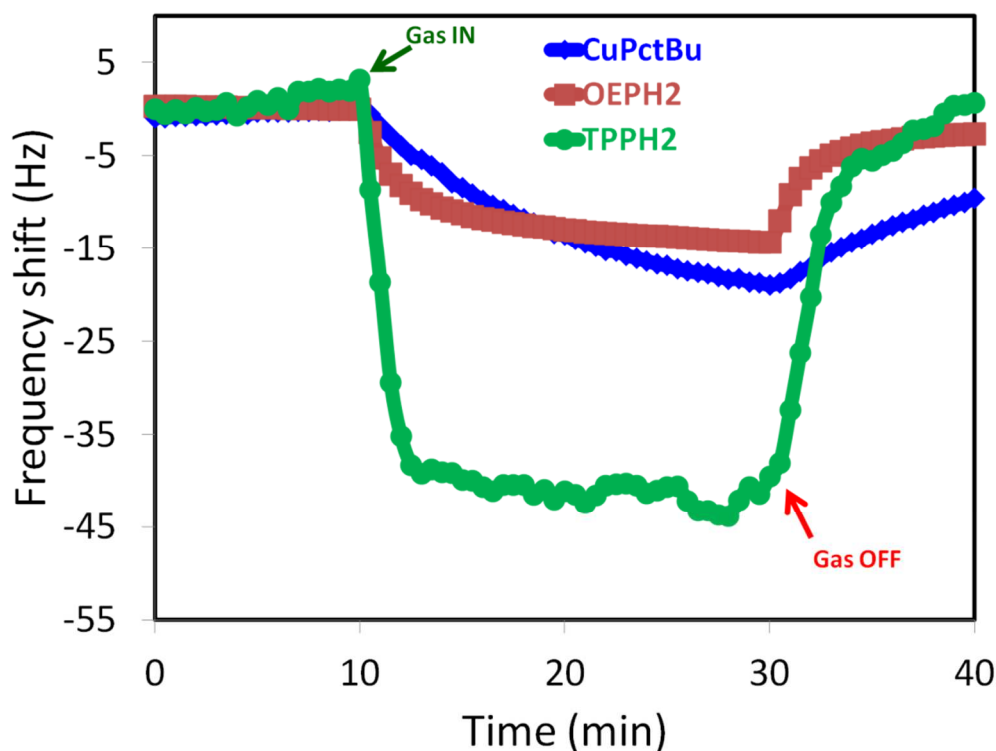


**Fig. 1: Frequency shift measured at room temperature (25°C) for macrocycles exposed to xylene (CuPctBu at 500 ppm , OEPH<sub>2</sub> at 450 ppm and TTPH<sub>2</sub> at 520 ppm) in dried air.**

Since the QCM transduction is a mass sensitive technique, therefore we normalized the frequency variation to the amount of deposited material for the discussion. The amount of deposited materials is calculated from the frequency difference before and after deposition using the sensitivity factor and the area of the electrode. The QCM response given in Hz/ng for xylene and benzene are displayed in Fig. 2A and Fig. 2B respectively. Data given in Fig. 2 show that the order of sensitivity is Xylene >> Benzene.

For benzene, CuPctBu and TTPH<sub>2</sub> are more sensitive than OEPH<sub>2</sub>, with CuPctBu showing the highest sensitivity. If we look at the structures of the macrocycles and that of the benzene while associating the potential interactions as detailed in Scheme 1 and Table 1, we can depict the following tendency: the CuPctBu and TTPH<sub>2</sub> which possess phenyl peripheral

groups are likely more sensitive to benzene than the OEPH<sub>2</sub> which contains only alkyl peripheral groups. These results seem to predict that: on the potentially existing interactions listed in Scheme 1 and Table 1, both are present, and  $\pi$ -alkyl interaction is potentially weaker than the  $\pi$ - $\pi$  interactions.

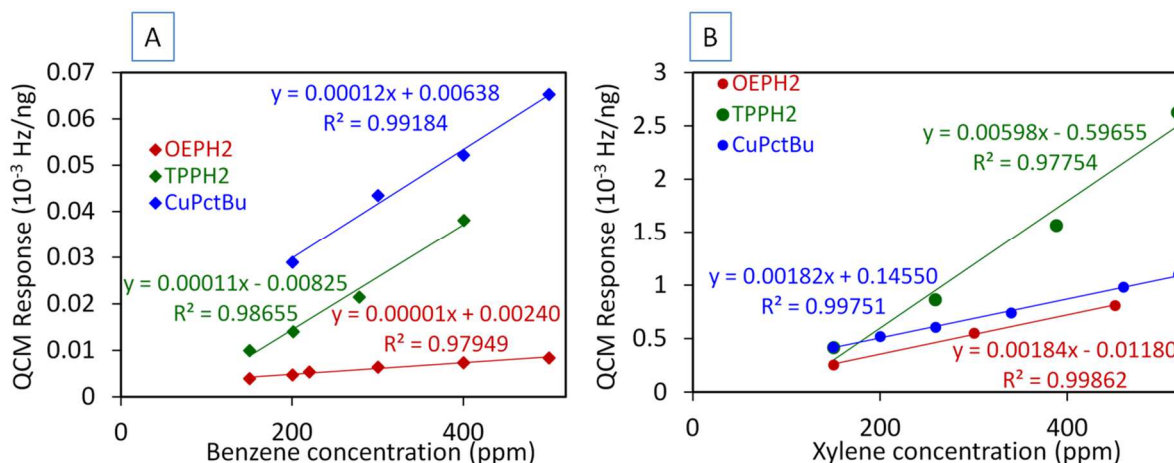


**Fig. 2: Calibration curves of QCM coated with macrocycles as function of the benzene (2A) and xylene (2B) concentrations at room temperature (25 °C). Equations corresponding to linearization by least square method are given.**

For xylene, a different trend is observed since TPPH<sub>2</sub> presents the highest sensitivity while CuPctBu and OEPH<sub>2</sub> present similar sensitivities with the lowest sensitivity value measured with the OEPH<sub>2</sub>. For the same reasons as given before, OEPH<sub>2</sub> is still the less sensitive material for xylene detection. Let's focus now on the difference between TPPH<sub>2</sub> and CuPctBu: the same explanation, relating the sensitivity with the peripheral groups previously discussed for benzene, applies also in the case of xylene. The major difference is coming from the structure of the VOCs bearing two methyl groups in the case of xylene while no methyl group is present for benzene. So upon adsorbing on the periphery of CuPctBu, the xylene will experience difficulty to adsorb easily because of the bulky tert-butyl groups surrounding the CuPctBu ring. As a result of such steric hindrance the sensitivity is lower for CuPctBu as compared to TPPH<sub>2</sub>.

We now add to our discussion the kinetics of adsorption/desorption measured during one exposure cycle. Kinetic parameters such as response time and recovery time can be determined from measurements reported in Fig. 1. Response time ( $\tau_{\text{resp}}$ ) and recovery time ( $\tau_{\text{rec}}$ ) are defined in the experimental section. Table 2 summarizes the response and recovery times depicted from the exposure sequences for the studied VOCs at room temperature.

**Table 2: Response and recovery times measured for the macrocycles exposed to BTX at room temperature (25 °C).**

	<b>XYLENE</b>		<b>BENZENE</b>		<b>TOLUENE</b>	
	$\tau_{\text{resp}}$ (min)	$\tau_{\text{rec}}$ (min)	$\tau_{\text{resp}}$ (min)	$\tau_{\text{rec}}$ (min)	$\tau_{\text{resp}}$ (min)	$\tau_{\text{rec}}$ (min)
<b>CuPctBu</b>	<b>15.5</b>	<b>30</b>	<b>4</b>	<b>5.5</b>	<b>14</b>	<b>20</b>
<b>OEPH<sub>2</sub></b>	<b>4</b>	<b>5</b>	<b>1.75</b>	<b>1.75</b>	<b>2.5</b>	<b>2</b>
<b>TPPH<sub>2</sub></b>	<b>6</b>	<b>4</b>	<b>1.5</b>	<b>2.75</b>	<b>2.5</b>	<b>1.75</b>

For the CuPctBu materials the most reactive VOC is xylene and the recovery time is the longest generating a slow kinetic of desorption. This is illustrated by the value  $\tau_{\text{rec}}$  of 30 min in the case of xylene (Fig. 1 and Table 2) while the recovery times are evaluated to 20 min for toluene and 5.5 min for benzene (Table 2). The fast desorption kinetics is recorded for benzene also with very weak sensitivity as compared to toluene and xylene.

For OEPH<sub>2</sub>, the most reactive VOC is also xylene as illustrated in the calibration curve in Fig. 2. The QCM response given in Hz/ng shows the same order of sensitivity Xylene > > Benzene. The desorption rate follows the same order than for CuPctBu with benzene giving the faster desorption. As previously observed for CuPctbu, the rapid desorption kinetics is recorded for benzene also with very weak sensitivity as compared to xylene. The same evolution is observed for TPPH<sub>2</sub> too (see calibration curves in Fig. 2 and

values in Table 2). If we include in the analysis the values for toluene [24] from the previous publication, the order of sensitivity is Xylene  $\geq$  Toluene  $\gg$  Benzene for TPPH<sub>2</sub> and Toluene  $\approx$  Xylene  $\gg$  Benzene for OEPH<sub>2</sub>.

Since the tendency follows inversely that of vapor pressure i.e. the lowest vapor pressure VOCs give the highest sensitivity and vice versa, one could imagine a linear relationship between sensitivity and vapor pressure. However, from the results, we can notice that responses for xylene are 50 times higher than those of benzene while the vapor pressure is only 10 times higher. This suggests no direct linear relationship between response and vapor pressure. The same analysis can be done for the couples xylene/toluene or benzene/toluene and we came to the same conclusion. These results show that even if the response follows the vapor pressure evolution, there is a non negligible contribution of the interaction on the sensor response.

### **3.1.3. Understanding the interaction mechanism between macrocycles and BTX**

Based on the analysis of the response of the TPPH<sub>2</sub> in interaction with benzene, an essential remark can be done: when the periphery are devoid of alkyl groups and that the only phenyl groups are present (TPPH<sub>2</sub>), the QCM sensors do not display a better sensitivity (Fig. 2A) nor rapid kinetics (Table 2). The same analysis for the OEPH<sub>2</sub> (bearing only alkyl peripheral group) in interaction with benzene show that, if only alkyl groups are present on the periphery, the QCM sensor displays the worst sensitivity (Fig. 2A) but a rapid kinetics (Table 2). From these results, it is obvious that the existence of  $\pi$ - $\pi$  interactions (from the periphery) as solely potential interaction is not sufficient to induce simultaneously better sensitivity and rapid kinetics. A similar analysis based on the results of OEPH<sub>2</sub> with benzene allows to state that if solely  $\pi$ -alkyl interactions are present then the adsorption is weak and the kinetics rapid. For the CuPctbu in interaction with benzene the same statement applies. CuPctBu present both phenyl (phthalimide) and alkyl (tert-butyl) groups on its periphery, therefore it is

more sensitive and the desorption is slower. From these analyses, it is clear that: i) in the case where the periphery is subject to  $\pi$ - $\pi$  interactions and additional  $\pi$ -alkyl interactions simultaneously (Scheme 1), the adsorption interaction is more favored and the desorption is too slow. ii) in situations where the periphery is subject to only  $\pi$ -interactions, the adsorption interaction is also favored and the desorption is slow. iii) in the case where the periphery is subject to only  $\pi$ -alkyl interactions, the adsorption interaction is less favored and the desorption is rapid.

It is worth noting that, for xylene as illustrated in Fig. 2B, CuPctBu which possesses both alkyl and phenyl peripheral groups is less sensitive than TTPH<sub>2</sub> which presents only phenyl peripheral groups. A reason for such a deviation is essentially attributed to the fact that tert-butyl moieties are bulky groups that can restrict the access to the peripheral active sites, if xylene molecules would adsorb on surfaces. This is not the case if the less bulky toluene is concerned. We found previously that the Pcs were more sensitive to toluene than the Por [24]. The differences can be attributed to steric effects which have not been taken into account in the prediction.

For VOCs without functional peripheral groups (benzene) where the only aromatic center is involved, the adsorption is weak and certainly the reactivity too. If the VOCs possess alkyl groups (methyl) on their periphery (case of toluene and xylene) then the interaction is reinforced. In terms of kinetics (recovery time in Table 2), the OEPH<sub>2</sub> which is less sensitive, present the most rapid kinetics compared to others MCs for all tested VOCs. This means that, if  $\pi$ - $\pi$  interactions are absent from the periphery, the interaction energy is not reinforced and as a consequence, the desorption is rapid.

Articles from the literature corroborate this tendency. In fact, Qiu *et al.* have reported on a contribution of peripheral alkyl chains on the stabilization of Pcs moieties. Their study illustrate indirectly that the alkyl groups in synergy with the  $\pi$ -interactions (van der Waals

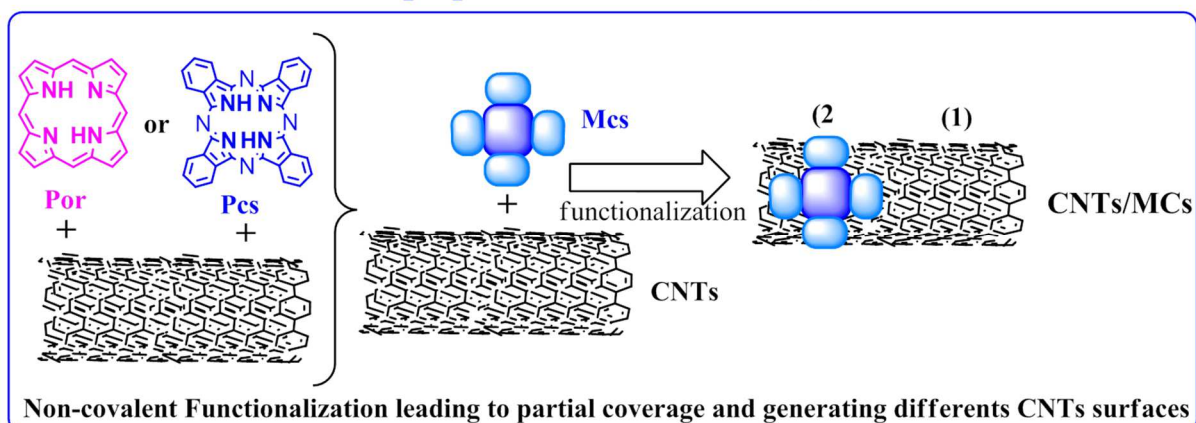
interactions) are important when macrocycles are involved in staking interactions [27]. Others studies confirm the importance of peripheral groups for VOCs adsorption on phthalocyanines [28]. A correlation between the desorption energy and the number of alkyl chains in the case of the desorption of n-alkanes from graphene [29] has been established. The authors found a linear relationship associating an increase in the number of alkyl chains to an increase in the desorption energy. The importance of peripheral groups on the adsorption of toluene [23] or benzene [30] on phthalocyanines has been also reported. Even if the  $\pi$ -interactions are likely the most probable interactions that can be encountered in the adsorption of VOCs on the aromatic center of the MCs, the presence of peripheral groups (methyl for VOCs and ethyl, tert-butyl or phenyl for the MCs) play an important and synergic role too.

### **3.2. Sensor performance of the hybrid CNTs/MCs exposed to BTX: understanding the CNTs/MCs reactivity towards VOCs**

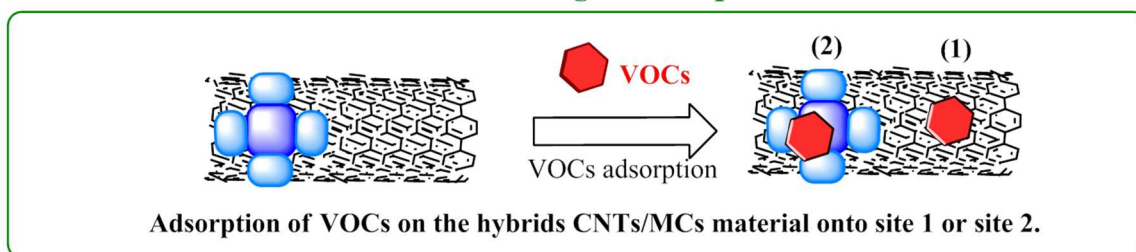
Scheme 2 represents the successive steps of functionalization (upper panel) and gas adsorption (lower panel) on hybrids materials, to illustrate both the material preparation and the gas adsorption possibilities. Hybrid materials were synthesized through non-covalent functionalization and as a result of the random functionalization occurs. Therefore, different CNTs area are revealed: Naked-CNTs surface (site 1) and occupied CNTs surface (site 2) (see upper panel of Scheme 2). This analysis stems from our previous observations on TEM images [24] combined with thermogravimetric analysis.

When we submit these hybrid materials to aromatic VOCs, the VOCs can potentially adsorb on both types of surfaces (site 1 et site 2; see lower panel of Scheme 2).

### *Material preparation / Functionalization*



### *Gas Sensing / Adsorption*



**Scheme 2: Representation of the functionalization of CNTs (upper panel) and VOCs adsorption on the hybrid materials (lower panel). Sites (1) define the Naked-CNTs surface and sites (2) define the occupied CNTs surface.**

So the discussion will be oriented through the potential interactions between VOCs and these two adsorption sites, their influence on the responses, the kinetics of desorption in relation with these two adsorption sites. At the end, the role played by the peripheral groups of the CNTs/MCs (ethyl, phenyl, etc.) and those of the VOCs (methyl for xylene and toluene) will be analyzed.

#### **3.2.1. Mass sensors responses and potential interactions**

##### **3.2.1.1. Mass sensor performances**

Fig. 3 shows an emphasis on adsorption/desorption profiles for the CNTs/OEPH<sub>2</sub> exposed to BTX. Here we will consider the adsorption as arising typically from physisorption phenomena. For the discussion, we focus on the QCM responses of the CNTs/OEPH<sub>2</sub> which presents the most interesting performances over all hybrid materials. The same analysis could



be made for CNTs/CuPctBu and CNTs/TPPH<sub>2</sub> (see Fig. S2 in supporting information). The sensors sensitivities for all the three hybrid materials submitted to VOCs are given in Table 3.

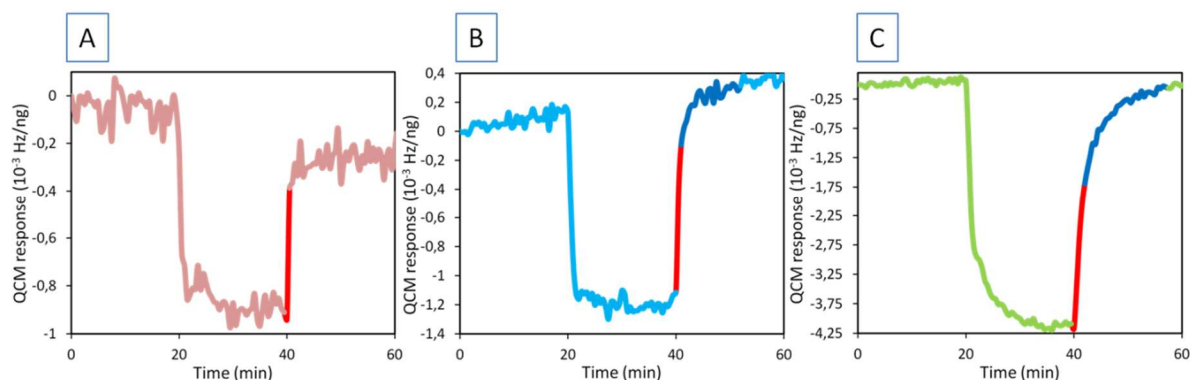


**Fig. 3: Focus on one exposure cycle of QCM response for the CNTs/OEPH<sub>2</sub> in reaction with 500 ppm benzene (A), Toluene (B) and Xylene (C). The red section represents the most rapid kinetics while the dark blue part in Fig. 3B and 3C display a slow and more persistent desorption. Experiments are performed at room temperature (25 °C).**

In Fig. 3, we can depicted two evolution of the desorption rates. The first one is highlighted in red color and represents the most rapid kinetics corresponding to a faster desorption. The second one is highlighted in blue color and represents a rather slow kinetics (at least for toluene and xylene) which indicates a slower and persistent desorption.

We found in Fig. 3 that the fast kinetics section lasts 30 seconds for benzene, 1.5 minutes for toluene and 2 minutes for xylene. This means that for the same material the order of kinetics of desorption is benzene more rapid than toluene which is more rapid than xylene. Similar trends are also observed for CNTs/CuPctBu and CNTs/TPPH<sub>2</sub>. From this analysis, it seems that desorption kinetics depends on the presence or absence of methyl groups of the VOCs whatever the CNTs/MCs materials.

**Table 3: Sensor sensitivities (S) calculated from the QCM response of the CNTs/MCs in the range 33 – 500 ppm and given in  $\mu\text{Hz}/\text{ng}/\text{ppm}$ .**

	Sensitivity to Xylene ( $\mu\text{Hz}/\text{ng}/\text{ppm}$ )	Sensitivity to Benzene ( $\mu\text{Hz}/\text{ng}/\text{ppm}$ )	Sensitivity to Toluene ( $\mu\text{Hz}/\text{ng}/\text{ppm}$ )
CNTs/CuPctBu	2	0.4	2
CNTs/OEPH <sub>2</sub>	10	2	4
CNTs/TPPH <sub>2</sub>	5	0.7	1

As displayed in Table 3, the order of sensitivity is xylene > toluene >> benzene for the CNTs/OEPH<sub>2</sub>. Mehdi et al. reporting on the adsorption of BTX on various carbonaceous materials (from CNTs to carbon fibers) illustrate the importance of the chemical composition of the surface more than the surface area. They found the same order for the BTX adsorption capacity (Xylene > Toluene > Benzene) independently of the nature of the carbon materials and the surface area [31].

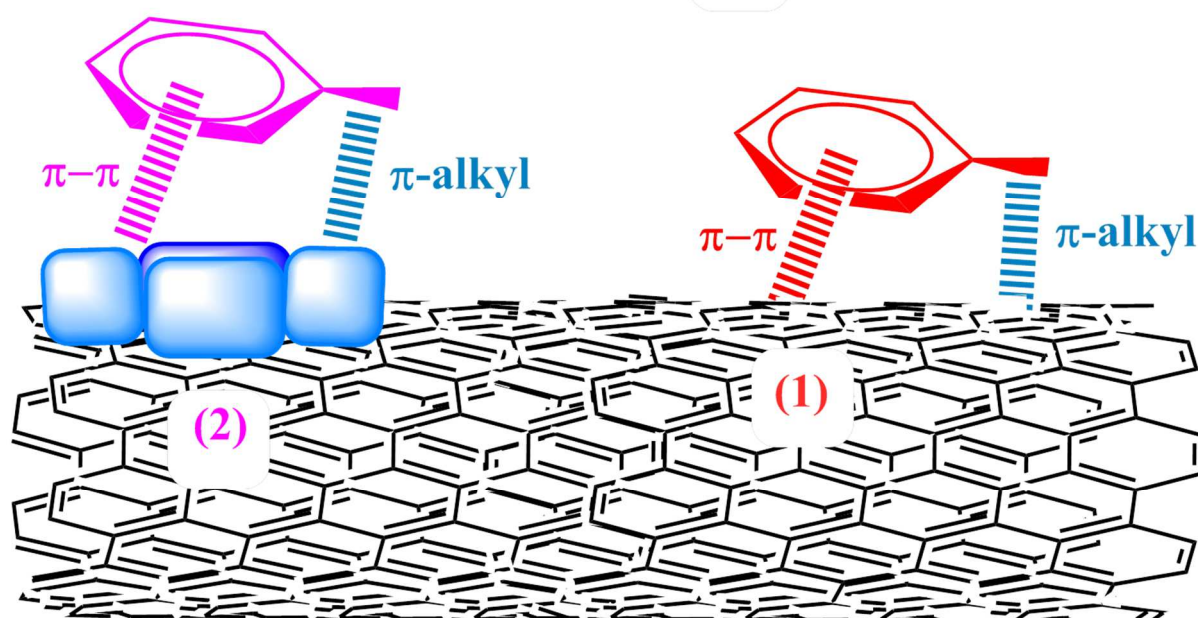
Of course since the VOCs have different vapor pressures the relationship between sensitivity and vapor pressure has to be considered. However if we comparatively analyze the sensitivity and vapor pressure, we can notice the following trend. The sensitivities (for all hybrid materials) to xylene are almost 5 times higher than those of benzene while the vapor pressure ratio between the two VOCs is 11 times higher. We came to the same conclusion between benzene and toluene where sensitivities to toluene are 1 (for CNTs/TPPH<sub>2</sub>), 2 (for CNTs/OEPH<sub>2</sub>) and 5 (for CNTs/CuPctBu) times higher than those of benzene while the vapor pressure is only 3 times higher. This suggests no direct linear relationship between response and vapor pressure.

### **3.2.1.2. Understanding the sensing mechanism between CNTs/MCs and BTX**

Analysis of the potential interactions between aromatics moieties and  $\pi$ -system assemblies suppose to define the different contributions on the interactions energy. Lazar et al. [32] working in Symmetry-adapted perturbation theory (SAPT) calculations indicated a predominance of dispersion contribution over the others energy contributions (electrostatics,

exchange repulsion and induction) to the interaction energy. A result which is further confirmed in other studies [33-34]. Wheeler et al. [34] goes even further and shows that this predominance of the dispersion is also valid for both endohedral and exohedral adsorption of aromatic (benzene) or non aromatic (cyclohexane) molecules on carbon nanotubes. Here we will focus on dispersion interactions as representing the dominant contribution to the interaction energy. But, we will also take into account substituent effects in  $\pi$ -stacking interactions as discussed by several authors [35-37].

### General adsorption of VOCs on sites 1 and 2 and potentials interactions



◀ : represents the peripheral alkyl groups on the VOCs;  
this representation is true for xylene and toluene while for benzene  
this later is absent.

**Scheme 3: Focus on the interaction of aromatic VOCs on the CNTs/MCs surfaces. Sites (1) and (2) refer to Naked-CNTs surface and MCs-occupied CNTs surface.**

Based on the structure analysis of the VOCs and the functionalizing moieties, we can presume the presence of both  $\pi$ -alkyl interactions and  $\pi$ - $\pi$  interactions as contributing to the kinetics of desorption. The final outcome of these considerations is highlighted in Scheme 3.

If we again analyze the Fig. 3 while referring to Scheme 3, we can find a correlation between kinetics of desorption and adsorption sites (1) or (2) in relation with the peripheral groups (substituents) of the VOCs: for benzene where the  $\pi$ -alkyl interactions are absent in sites (1), we recorded the most rapid desorption and the lowest sensitivity. We deliberately assume that adsorption on CNTs sites 1 for benzene is essentially of  $\pi$ - $\pi$  type. In fact, CH- $\pi$  interactions involving T-shaped configuration where benzene molecule interacts with an benzene center through CH- $\pi$  interaction, is less stable than any of the stacking interaction [38]. For toluene and xylene where the  $\pi$ -alkyl interactions are present in sites (1), we noticed a rather slowdown of the desorption and higher sensitivities. This result has to be correlated with the nature of the VOCs more than the nature of functionalizing moieties.

So if we combined the analysis of Fig. 3 on the existence of two desorption rates and the adsorption scheme depicted in Scheme 3, we came to the conclusion that: i) the rapid evolution (red line in Fig. 3) suggests a desorption from sites 1; ii) while the remaining part of the desorption profile in Fig. 3 (highlighted in blue color) is a contribution of the desorption of the VOCs from the functionalized CNTs parts (sites 2).

To understand the desorption kinetics it is necessary look insight the interface and state that VOCs with weak affinity to the surface will leave first the surface and those with strong affinity will leave later the surface of the sensing material. Initially the adsorption happens on both sites as illustrated on Schemes 2 and 3; however, depending on the chemical environment of the VOCs (methyl groups for toluene or xylene) a reinforcement of the native  $\pi$ - $\pi$  interaction through the existence of additional  $\pi$ -alkyl interaction takes place. This is the case for xylene and toluene. These statements are summarized in Table 4.

In the case of benzene the additional  $\pi$ -alkyl interactions are absent and the only  $\pi$ - $\pi$  interactions ensure the adsorption on site 1 (CNTs surface). As a consequence, benzene presents the weakest interactions with the CNTs/MCs and the desorption is rapid. Toluene

and xylene bear methyl groups that can participate to reinforce native  $\pi$ - $\pi$  interaction through additional  $\pi$ -alkyl interaction. As a consequence they are more sensitive and desorption takes place more slowly. This result corroborates with the findings of Lee et al. [39] evaluated in stacked configuration. In fact, they stated that, upon substitution on the benzene ring (toluene and xylene), the aromatic-aromatic interaction is enhanced through a contribution (interaction) from the benzene ring and the substituent of the other ring [39].

**Table 4: Relative strength of the potential interactions and their influence on the kinetic of desorption.**

	$\pi$ -alkyl interactions (lonely)	$\pi$ - $\pi$ interaction (lonely)	$\pi$ - $\pi$ interaction + $\pi$ -alkyl interaction
Relative strength	Weak	Moderate	Strong
Desorption	Rapid	Rapid	Slow
Synergetic Contribution	-	-	Reinforcement of the $\pi$ - $\pi$ interaction

If  $\pi$ - $\pi$  interactions are the only existing interaction, we have a moderate interaction, but if both  $\pi$ - $\pi$  and  $\pi$ -alkyl interactions coexist we have a stronger interaction due to the reinforcement of the  $\pi$ - $\pi$  interactions by the  $\pi$ -alkyl interactions (Table 4). From this analysis we can expect that adsorption on sites 1 would be reinforced for toluene and xylene bearing methyl groups on their periphery (substituent). For adsorption on sites 2, a part from CNTs/TTPH<sub>2</sub> (in interaction with benzene), the  $\pi$ - $\pi$  interactions are overall reinforced by the presence  $\pi$ -alkyl interactions.

Assuming that  $\pi$ - $\pi$  interactions exist in such materials in their interactions with aromatic VOCs, the gas/material interaction can be witnessed as a synergy of interactions

associating alkyl-alkyl and  $\pi$ -alkyl interaction as well as  $\pi$ - $\pi$  interaction. Our assumption corroborates with the finding of Wheeler et al. [40] who advises to take into account direct interactions involving the substituents.

So both the analyses detailed in sections 3.2.1.1 (kinetics and sensitivity) and 3.2.1.2 (dispersion interactions) confirms that desorption relies on the presence or absence of methyl groups on the periphery of the VOCs, independently of the CNTs/MCs materials.

### 3.2.2. Resistive sensors performances

In the resistive sensors, the adsorption and desorption profile are relatively identical for a defined gas or vapor type. The resistance increases when submitted to BTX Gases. For this reason, we present here the result of the most sensitive CNTs/MCs matrix namely CNTs/CuPctBu towards VOCs as given in Fig. 4. The resistive sensors responses are given as resistance variation ( $\Delta R$ ) representing the difference between resistance under air zero ( $R_0$ ) and resistance under VOCs vapors ( $R_{Gas}$ ) i.e. ( $\Delta R = R_{Gas} - R_0$ ). However, in contrast to QCM responses, the response time and recovery time are more difficult to assess for the resistive sensors because of the fluctuation of the resistance and incomplete recovery under air zero. We can also define here two desorption profiles as in the case of mass sensors.

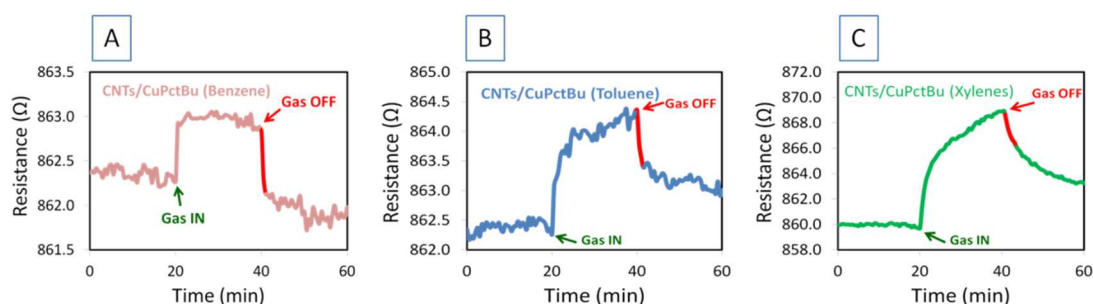


**Fig. 4:** Focus on one cycle of exposure of resistive sensor response given as resistance for the CNTs/CuPctBu in reaction with benzene (A), toluene (B) and xylene (C). The red part of the curve represents the most rapid kinetics between 30 seconds (benzene), 1.5 minutes (toluene) and 2 minutes (xylene). Experiments are performed at room temperature (25 °C).

In principle, adsorption of the VOCs on hybrid materials are identical whatever the transducer (QCM or resistive). For this reason, the Scheme 2 remains valid in terms of adsorption and potential interactions. The mechanism of sensing is however different, since for the resistive sensor, adsorption and simultaneously charge transfer are both necessary to observe a sensor signal. It is also worthy to note that in the case of VOCs without redox properties like BTX, the charge transfer is difficult to achieve. However charges trapping [41] due to adsorption, change in the CNT/CNTs interface [42] and/or a modulation of the inter-tubes electron interaction [43] can induce changes on the conductivity once vapors molecules are adsorbed on CNTs surface.

Because of the very weak interaction between alkyl moieties and CNTs surface or MCs surface, the conductivity is not enhanced through  $\pi$ -alkyl interactions as encountered in the QCM results. Furthermore, the alkyl groups do not allow significant electronic exchanges with CNTs surface. As an example, submitting hexane vapor to the CNTs/MCs surface does not give any signal during the resistive sensing experiments.

The adsorption of VOCs on the CNTs results generally in a weaker contribution on the electronic properties of CNTs materials [44-45]. Theoretical calculations on benzene adsorption on CNTs [46] or graphene [33] also support this conclusion. All this information reveals that, although the  $\pi$ - $\pi$  interactions dominate the adsorption interaction, they do not give rise to significant electrical contribution; neither do the  $\pi$ -alkyl interaction which produces no electronic exchange. This conclusion is valid for adsorption on sites 1 (Scheme 2).

The functionalization affords new adsorption sites, but the organic macrocycles have very low conductivity so that generally higher resistivity is measured. We have also seen that after functionalization electrical contribution from the CNTs dominates the whole electrical properties. This means that even if the gaseous molecules adsorbed on the functional moieties

(sites 2 in Scheme 2) their electrical contribution will be negligible because of the quasi-insulating nature of the functional moieties and the lack of electronic exchange. Therefore we can assume that the adsorption of gaseous molecules on the functional peripheral groups contribute to a weaker extent to the resistive response. The measured resistive response can be potentially attributed to contribution from the direct adsorption of the VOCs on the naked CNTs surface (sites 1 in Scheme 2). As a consequence, the kinetics is a signature of the peripheral groups of the VOCs (more than that of the peripheral groups of the MCs), and this is illustrated in the resistive response profile given in Fig. 4.

We performed sensing experiments using simultaneously mass and resistive transductions. A cross analysis of the performances based on the use of double transduction mode allow to highlight a general trend that is depicted from the values given in Table 5.

**Table 5: Response and recovery times for the mass and resistive sensors based on the CNTs/MCs materials at room temperature (25 °C). NA: Not Available; because of the weak and unstable responses. NB: the pristine CNTs do not present stables and reliable responses and are therefore not included.**

QCM						
	XYLENES RESPONSES		BENZENE RESPONSES		TOLUENE RESPONSES	
	$\tau$ resp (min)	$\tau$ rec (min)	$\tau$ resp (min)	$\tau$ rec (min)	$\tau$ resp (min)	$\tau$ rec (min)
CNTs/CuPctBu	4.5	7	1.5	1	3	3.5
CNTs/OEPH <sub>2</sub>	5	5	2	1	2	2
CNTs/TPPH <sub>2</sub>	4	8	1.5	2	2	3.5

Resistive						
	XYLENES RESPONSES		BENZENE RESPONSES		TOLUENE RESPONSES	
	$\tau$ resp (min)	$\tau$ rec (min)	$\tau$ resp (min)	$\tau$ rec (min)	$\tau$ resp (min)	$\tau$ rec (min)
CNTs/CuPctBu	14	30	0.75	1.75	4.5	8
CNTs/OEPH <sub>2</sub>	14	16	NA	NA	4	10.5
CNTs/TPPH <sub>2</sub>	10.5	17	0.5	1	3	6.5

Apart from benzene, the mass sensors give the most rapid kinetics as compared to the resistive sensors. This is essentially attributed to the action of the VOCs on the sensing layer. While the mass transduction is only sensitive to adsorption, the resistive transduction will display a signal if two conditions (adsorption and subsequent charge transfer or phenomena



leading to conductivity changes) are fulfilled. However, in terms of sensitivity towards the VOCs, the classification is always the same (Xylene  $\geq$  Toluene  $>$  Benzene) showing that the way one VOC interacts with the hybrid materials is identical whatever the transduction.

### 3.3. Fitting of the desorption kinetics with mathematical function

We can deepen the analysis of the desorption using mathematical function fitting. In fact, if we look at the QCM response (taking for example any of the CNTs/MCs materials) we find a response profile similar to that presented in Fig. 5 (and previous figures too). If we concentrate on a section of the desorption profile chosen arbitrarily (10 minutes before end of the submission, until 20 minutes after), we got the red box delimitation in Fig. 5A. If we focus carefully on the projection of the red box, we can identify a sigmoid curve as given in Fig. 5B.

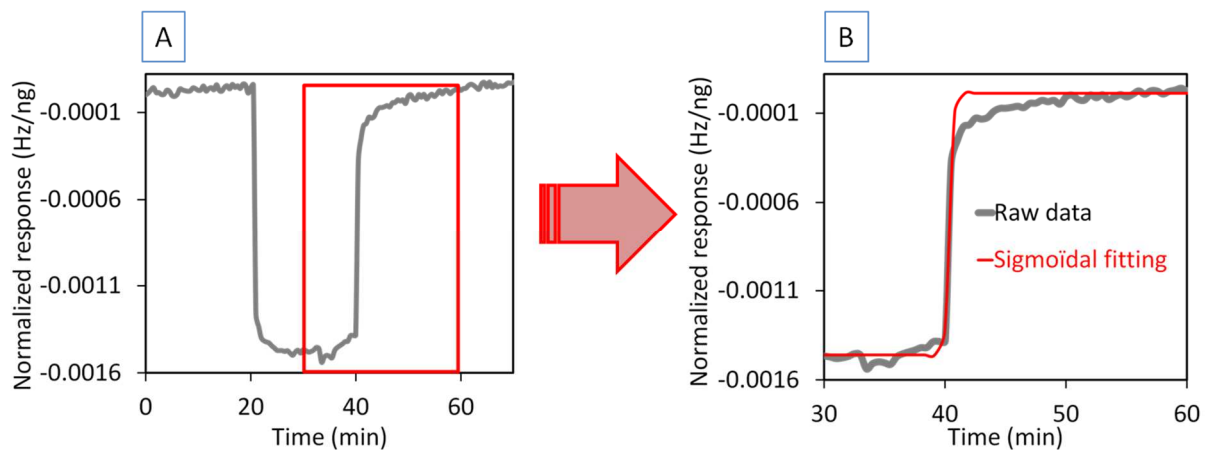


**Fig. 5: Focus one section of dynamic QCM response of the CNTs/OEPH<sub>2</sub> sensor to benzene (A) and projection of the red frame (the sigmoid section) mathematically fitted ( $R^2=0.997$ ) with a sigmoidal function (B).**

The sigmoid function is described by (Eq. 1):

$$Y = \frac{(A1 - A2)}{(1 + \exp((x - x0) / dx))} + A2 \quad (\text{Eq.1})$$

an illustration is given in Fig. S4 (see supplementary information)

where A1 is initial value and A2 the final value ;  $x_0$  = the value at 50% of the amplitude;

$dx$  = the width, a constant that determines the curvature and give insight into the kinetics.

So if we fit the raw data from the QCM sensor response, we obtain the curves as displayed in Fig. 5B with the raw data and their corresponding sigmoidal fitting. The results of such a mathematical fitting are given in Table 6 for the CNTs/MCs. For the resistive sensors the sigmoid fitting was not adapted because of their dynamic response which do not fit correctly to a sigmoid form. Even if some regression coefficients ( $R^2$ ) in Table 6 are critical, we can depict some interesting features for the CNTs/MCs: the lowest dx values are recorded for benzene whatever the material used; intermediate values of dx are recorded for toluene while higher dx values are obtained for xylene.

**Table 6: Summary of the sigmoidal fitting for the CNTs/MCs giving the width (dx) and the corresponding correlation coefficient ( $R^2$ ).**

	Benzene		Toluene		Xylene	
	dx	$R^2$	dx	$R^2$	dx	$R^2$
<b>CNTs/CuPctBu</b>	0.134	0.970	0.369	0.991	1.748	0.978
<b>CNTs/OEPH<sub>2</sub></b>	0.023	0.938	0.293	0.979	1.404	0.981
<b>CNTs/TPPH<sub>2</sub></b>	0.139	0.935	0.324	0.982	2.156	0.975

Considering that dx traduces the celerity of the function to go from the floor (A1) to the ceiling (A2), we can state that the lower the dx values are the more rapid the desorption is. So the analysis of the dx values as given in Table 6 highlights again the fact that benzene desorbs more rapidly than toluene and xylene. It is worth noting that in the case of xylene, which presents the highest dx values over all VOCs, both  $\pi$ - $\pi$  interaction and  $\pi$ -alkyl interactions coexist. Taking into account that point, we can anticipate that for the comparison of BTX response exposed to the same material the range of the dx value can predict strength of the interaction. These results corroborate with the precedent analyses detailed on section 3. 2 and show again that the nature of the VOCs dictate desorption kinetics for CNTs/MCs.

The functionalized CNTs materials generally form mats or aggregates once they are layered on device supports. Therefore the sensing layers can present surface irregularities, porosity and so one, that can slow down the desorption or induce different desorption rate. Since both the kinetics and the response can be dependent of the exposure time, we explore in a experiment the effect of the submission duration on both the response and desorption kinetics.

### 3.4. Influence of the exposure time on the response and the desorption kinetics

We performed an experiment consisting in increasing the submission time from 5 minutes to 30 minutes by steps of 5 minutes while keeping the recovery duration constant. The results are displayed in Fig. 6 and concern the CNTs/OEPH<sub>2</sub> submitted to the same concentration of toluene.

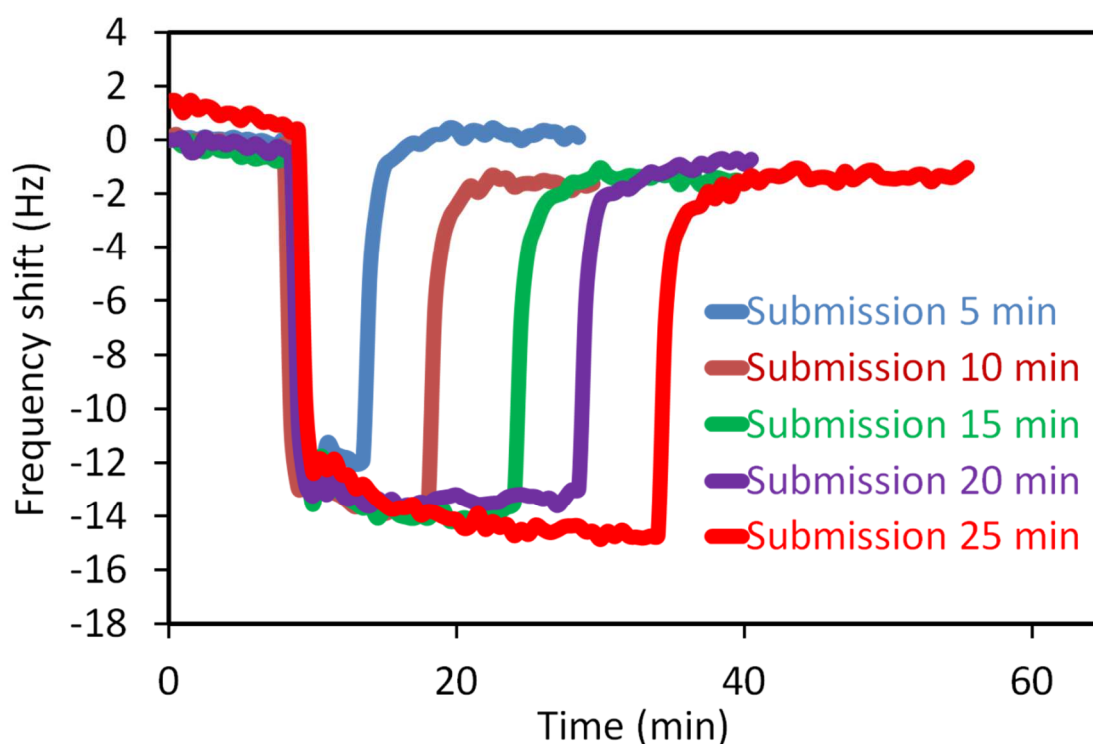


**Fig. 6: Sequential submission exposure of toluene to CNTs/OEPH<sub>2</sub> upon variation of the submission duration.**

The results show that the response amplitude is almost 12 Hz for submission duration of 5 minutes while it is almost identical (~ 15 Hz) when submission durations are increased

consecutively from 10 to 25 minutes. This result is a proof that the interactions are mainly localized on the surface and that diffusion into the volume is limited. The kinetics of desorption is almost identical with response and recovery times values averaging the 2 minutes whatever the submission duration. These results are concomitant with exchanges essentially localized on the surface and with a limited contribution of the diffusion into the volume.

### **3.5. Influence of the relative humidity on the room temperature sensor response**

It is known that CNTs materials are moisture sensitive, so since the sensing performance we are describing, are realized at room temperature, we included a small section dealing with the humidity effect. The effect of relative humidity on the gas sensor response has been evaluated and the results presented in Fig. 7 for the case of CNTs/OEPH<sub>2</sub> under BTX vapor exposure. The same tendency is observed for the CNTs/CuPctBu and CNTs/TPPH<sub>2</sub>. Example of frequency shift variation under toluene for CNTs/OEPH<sub>2</sub> at different humidity environment is given in Fig. S5 (see supporting information). For both the QCM and resistive devices we observed an decrease in the sensor response of the CNTs/MCs with increasing relative humidity (RH) whatever the vapors detected.

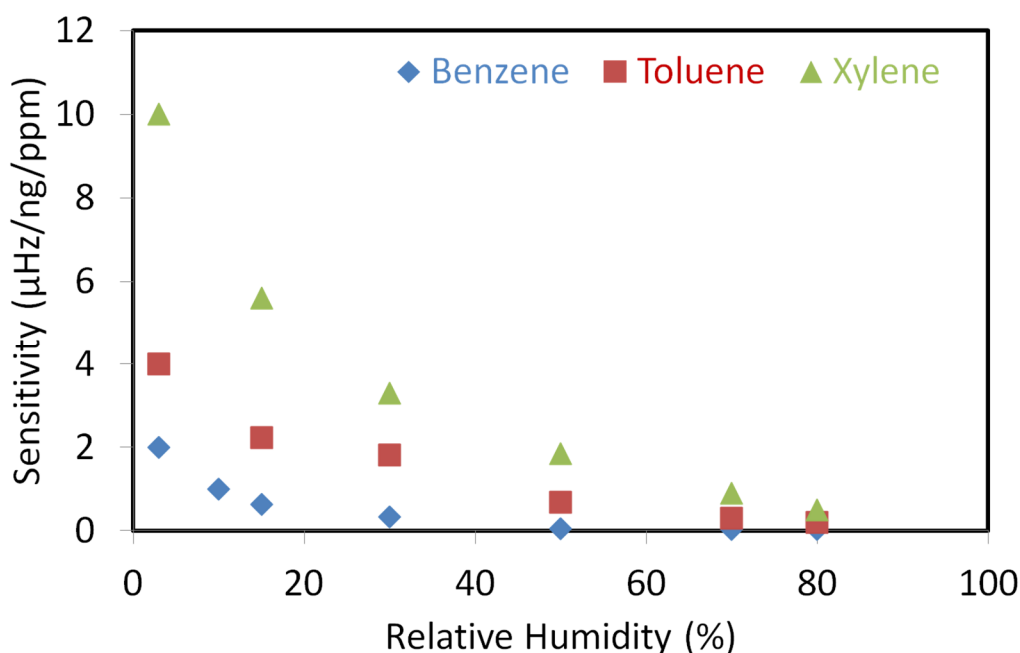


**Fig. 7: Sensitivity of the CNTs/OEPH<sub>2</sub> materials as function of the relative humidity for BTX exposure.**

The measurement at higher relative humidity conditions (>70% RH) lead to very poor sensitivity of the sensors, while measurement approaching the dried conditions (3-30% RH) present the highest sensitivity. The fact that humidity produced perturbation on the CNTs-based sensing materials is not surprising since CNTs themselves can be used as sensing material for humidity sensing meaning that the CNTs surface is humidity sensitive. This is certainly due to carbon impurities or defects which are reactive sites that can be subject to hydrogen bonding. A close focus on the Fig. 7 allows to realize that the sensor sensitivity variation induced by 50% RH is about 5 times lower than the sensor sensitivity in dried condition (3% RH) for xylene and toluene while this value is 40 times lower for benzene. This variation is not negligible. This means that if high humidity environment (higher than 50% RH) are intended then it might be necessary to compensate the signal variation due to humidity in order to correctly used the sensor device with accuracy.

### 3.6. Study of the long-term stability on the room temperature sensor response

In addition to studies on the influence of the relative humidity, the long-term stability has been checked. Therefore, sensors response measurement to 500 ppm toluene was carried out to investigate this parameter and the results are displayed in Fig. S6. We can see in Fig. S6 that generally (for the CNTs/MCs) the response deviates from that recorded at the beginning (first day) within the 10 first days and remains almost stable above the 10 first days. This deviation corresponds to 8% loss of the initial response for CNTs/OEPH<sub>2</sub> and 12.5 % for CNTs/CuPctBu and 30% for CNTs/TPPH<sub>2</sub>. This is due to the fact that at the beginning some interaction sites experience irreversible reactions (like chemisorptions leading not only to a baseline drift, but also to signal variation from successive exposures). These 10 first days of experience can be accounted for the conditioning period. In the measurements done after the conditioning period (> 10 – 20 days of experiments) at the same conditions and concentration range, the sensors responses are quite repeatable. In fact, after this conditioning period, the irreversible interaction sites are almost saturated and the remaining reversible interaction sites lead to stable and almost repeatable responses.

The functionalization brings sensitivity to the CNTs hybrid materials which results from a contribution of the functional moieties on the enhancement of the surface reactivity. This study reveals that even if the  $\pi$ – $\pi$  interactions are dominating the gas material interaction, the peripheral groups of the VOCs play an important role on the gas material interaction. In many case studies concerning the phthalocyanines, the peripheral groups are intended to solve the solubility problem, and allow the preparation of hybrid materials by means of functionalization process in adequate solvent. If these alkyl chains are well identified as good solubilizing groups, any adsorption/interaction with these groups will give rise to contribution on the mass signal output (frequency shift) but the electrical signal (resistance variation) will remain almost unaffected. This result is a proof that the adsorption is closely related to the interaction energy more than the size of the different of the VOCs. Keep in mind that the

interaction energy is also related to the nature of the interacting forces ( $\pi$ - $\pi$  or alkyl- $\pi$  etc.) and hence closely related to the surface composition. From this point, it is obvious that the selectivity issue will be addressed by focusing on the surface chemistry in relation with the peripheral groups of the VOCs.

#### **4. Conclusion**

In this article we have studied sensing materials made of organic macrocycles (MCs) and carbon nanotubes functionalized with MCs (CNTs/MCs) to elucidate the interaction mechanisms when they are exposed to BTX vapors. Results from the MCs (alone) analysis allow some highlights: i) basically  $\pi$ -interactions between the VOCs and the macrocycles are overall present (Table 2); ii) the presence of alkyl groups contribute to reinforce the  $\pi$ -interactions through substituent effects; iii) this reinforcement is due to the sum of  $\pi$ - $\pi$  interactions,  $\pi$ -alkyl interactions and alkyl interactions if they work collectively in a synergic way. The results based on macrocycles responses show that the functional peripheral groups of the MCs play an important role on defining the kinetic of desorption. However, after functionalization the key factor for defining the mechanism is the functional peripheral groups of the VOCs (methyl). In terms of sensitivity, the functionalization increases the sensitivity by incorporation of new and sensitive interaction sites into the CNTs matrix. Using a double transduction mode helps to state that even if adsorption on the high surface area CNTs materials is overall possible, the charge transfer between the aromatic VOCs and the hybrid materials remains weak. The mass sensors is sensitive to all adsorption sites and present different profile according to the sites where the adsorption takes place (sites 1 or 2). But the impact of the alkyl groups on the VOCs (for xylene and toluene) is of paramount importance for the kinetics of the surface reaction and will be certainly the key for the selectivity.

## Supplementary material

Figures S1 contains QCM sensors responses upon benzene exposure for macrocycles. Figures S2 and S3 contain QCM sensors responses upon xylene exposure for CNTs/CuPctBu and CNTs/TPPH<sub>2</sub>. Fig. S4 shows the equation and the curve illustrating the sigmoid function. Fig. S5 shows an example of one submission cycle illustrating the frequency decrease recorded for the CNTs/OEPH<sub>2</sub> under different humidity relative conditions (13-80% RH). Fig. S6 contains the long-term stability results. This material is available free of charge via the journal homepage.

## Acknowledgements

This work has been sponsored by the French government research program "Investissements d'Avenir" through the IDEX-ISITE initiative 16-IDEX-0001 (CAP 20-25), the IMobS3 Laboratory of Excellence (ANR-10-LABX-16-01) and the RobotEx Equipment of Excellence (ANR-10-EQPX-44). This research was also financed by the European Union through the Regional Competitiveness and Employment program -2014-2020- (ERDF – AURA region) and by the AURA region.

## References

- [1] E. Llobet, Gas sensors using carbon nanomaterials: A review, *Sens. Actuators, B*, 179(2013) 32-45.
- [2] M. Penza, G. Cassano, P. Aversa, F. Antolini, A. Cusano, M. Consales, et al., Carbon nanotubes-coated multi-transducing sensors for VOCs detection, *Sens. Actuators, B*, 111-112(2005) 171-180.
- [3] G. Bottari, G. de la Torre, D.M. Guldi, T.s. Torres, Covalent and Noncovalent Phthalocyanine–Carbon Nanostructure Systems: Synthesis, Photoinduced Electron Transfer, and Application to Molecular Photovoltaics, *Chem. Rev.*, 110(2010) 6768-6816.
- [4] R.G. Amorim, A. Fazzio, A.J.R. da Silva, A.R. Rocha, Confinement effects and why carbon nanotube bundles can work as gas sensors, *Nanoscale*, 5(2013) 2798-2803.
- [5] G. Guo, F. Wang, H. Sun, D. Zhang, Reactivity of silicon-doped carbon nanotubes toward small gaseous molecules in the atmosphere, *Int. J. Quantum Chem.*, 108(2008) 203-209.
- [6] S.B. Fagan, E.J.G. Santos, A.G. Souza Filho, J. Mendes Filho, A. Fazzio, Ab initio study of 2,3,7,8-tetrachlorinated dibenzo-p-dioxin adsorption on single wall carbon nanotubes, *Chem. Phys. Lett.*, 437(2007) 79-82.
- [7] M. Penza, R. Rossi, M. Alvisi, D. Valerini, E. Serra, R. Paolesse, et al., Metalloporphyrins-functionalized carbon nanotube networked films for room-temperature VOCs sensing applications, *Procedia Chem.*, 1(2009) 975-978.



- [8] A.D. Rushi, K.P. Datta, P.S. Ghosh, A. Mulchandani, M.D. Shirsat, Selective Discrimination among Benzene, Toluene, and Xylene: Probing Metalloporphyrin-Functionalized Single-Walled Carbon Nanotube-Based Field Effect Transistors, *J. Phys. Chem. C*, 118(2014) 24034-24041.
- [9] J.Y. Chin, C. Godwin, E. Parker, T. Robins, T. Lewis, P. Harbin, et al., Levels and sources of volatile organic compounds in homes of children with asthma, *Indoor Air*, 24(2014) 403-415.
- [10] G. de Gennaro, G. Farella, A. Marzocca, A. Mazzone, M. Tutino, Indoor and Outdoor Monitoring of Volatile Organic Compounds in School Buildings: Indicators Based on Health Risk Assessment to Single out Critical Issues, *Int. J. Environ. Res. Public Health*, 10(2013) 6273-6291.
- [11] C. Chipot, R. Jaffe, B. Maigret, D.A. Pearlman, P.A. Kollman, Benzene Dimer: A Good Model for  $\pi$ - $\pi$  Interactions in Proteins? A Comparison between the Benzene and the Toluene Dimers in the Gas Phase and in an Aqueous Solution, *J. Am. Chem. Soc.*, 118(1996) 11217-11224.
- [12] G. de la Torre, G. Bottari, U. Hahn, T. Torres, Functional Phthalocyanines: Synthesis, Nanostructuration, and Electro-Optical Applications, in: J. Jiang (Ed.) *Functional Phthalocyanine Molecular Materials*, Springer Berlin Heidelberg, 2010, pp. 1-44.
- [13] S.p. Campidelli, B. Ballesteros, A. Filoramo, D.D.a. Díaz, G. de la Torre, T.s. Torres, et al., Facile Decoration of Functionalized Single-Wall Carbon Nanotubes with Phthalocyanines via "Click Chemistry", *J. Am. Chem. Soc.*, 130(2008) 11503-11509.
- [14] D.M. Guldi, I. Zilbermann, A. Gouloumis, P. Vázquez, T. Torres, Metallophthalocyanines: Versatile Electron-Donating Building Blocks for Fullerene Dyads, *J. Phys. Chem. B*, 108(2004) 18485-18494.
- [15] A. Kumar, J. Brunet, C. Varenne, A. Ndiaye, A. Pauly, M. Penza, et al., Tetra-tert-butyl copper phthalocyanine-based QCM sensor for toluene detection in air at room temperature, *Sens. Actuators, B*, 210(2015) 398-407.
- [16] J. Rossignol, G. Barochi, B. de Fonseca, J. Brunet, M. Bouvet, A. Pauly, et al., Development of Gas Sensors by Microwave Transduction with Phthalocyanine Film, *Procedia Eng.*, 47(2012) 1191-1194.
- [17] I. Leray, M.-C. Vernières, C. Bied-Charreton, Porphyrins as probe molecules in the detection of gaseous pollutants: detection of benzene using cationic porphyrins in polymer films, *Sens. Actuators, B*, 54(1999) 243-251.
- [18] J.A.J. Brunink, C. Di Natale, F. Bungaro, F.A.M. Davide, A. D'Amico, R. Paolesse, et al., The application of metalloporphyrins as coating material for quartz microbalance-based chemical sensors, *Anal. Chim. Acta*, 325(1996) 53-64.
- [19] A. D'Amico, C. Di Natale, R. Paolesse, A. Macagnano, A. Mantini, Metalloporphyrins as basic material for volatile sensitive sensors, *Sens. Actuators, B*, 65(2000) 209-215.
- [20] A. Macagnano, E. Sgreccia, R. Paolesse, F. De Cesare, A. D'Amico, C. Di Natale, Sorption and condensation phenomena of volatile compounds on solid-state metalloporphyrin films, *Sens. Actuators, B*, 124(2007) 260-268.
- [21] E. Kaki, A.R. Özkaya, A. Altındal, B. Salih, Ö. Bekaroğlu, Synthesis, characterization, electrochemistry and VOC sensing properties of novel metallophthalocyanines with four cyclohexyl-phenoxyphthalonitrile groups, *Sens. Actuators, B*, 188(2013) 1033-1042.
- [22] Y. Çimen, E. Ermiş, F. Dumludağ, A.R. Özkaya, B. Salih, Ö. Bekaroğlu, Synthesis, characterization, electrochemistry and VOC sensing properties of novel ball-type dinuclear metallophthalocyanines, *Sens. Actuators, B*, 202(2014) 1137-1147.
- [23] S. Şahin, S. Altun, A. Altındal, Z. Odabaş, Synthesis of novel azo-bridged phthalocyanines and their toluene vapour sensing properties, *Sens. Actuators, B*, 206(2015) 601-608.

- [24] A. Ndiaye, P. Bonnet, A. Pauly, M. Dubois, J. Brunet, C. Varenne, et al., Noncovalent Functionalization of Single-Wall Carbon Nanotubes for the Elaboration of Gas Sensor Dedicated to BTX Type Gases: The Case of Toluene, *J. Phys. Chem. C*, 117(2013) 20217-20228.
- [25] A.L. Ndiaye, J. Brunet, C. Varenne, A. Pauly, Functionalized CNTs-Based Gas Sensors for BTX-Type Gases: How Functional Peripheral Groups Can Affect the Time Response through Surface Reactivity, *J. Phys. Chem. C*, 122(2018) 21632-21643.
- [26] G. Sauerbrey, Verwendung von Schwingquarzen zur Wägung dünner Schichten und zur Mikrowägung, *Zeitschrift für Physik A Hadrons and Nuclei*, 155(1959) 206-222.
- [27] X. Qiu, C. Wang, S. Yin, Q. Zeng, B. Xu, C. Bai, Self-Assembly and Immobilization of Metallophthalocyanines by Alkyl Substituents Observed with Scanning Tunneling Microscopy, *J. Phys. Chem. B*, 104(2000) 3570-3574.
- [28] A. Kumar, J. Brunet, C. Varenne, A. Ndiaye, A. Pauly, Phthalocyanines based QCM sensors for aromatic hydrocarbons monitoring: Role of metal atoms and substituents on response to toluene, *Sens. Actuators, B*, 230(2016) 320-329.
- [29] L. Elisa, K.K. Emma, L. Marcus, O. Dimitri, D.R. Jonatan, S. Elsebeth, Desorption of n-alkanes from graphene: a van der Waals density functional study, *Journal of Physics: Condensed Matter*, 24(2012) 424212.
- [30] H.E. Alamin Ali, N. Can, S. Altun, Z. Odabas, The effects of substituent position on kinetics of benzene vapour adsorption onto 3-phenylphenoxy substituted metal-free and metallo-phthalocyanines thin films, *Dalton Transactions*, 45(2016) 16922-16930.
- [31] Mehdi Jahangiri, Seyed Jamaledin Shahtaheri, Javad Adl, Alimorad Rashidi, Hossein Kakooei, Abbas Rahimi Forushani, et al., The Adsorption of benzene, toluene and xylenes (BTX) on the carbon nanostructures: The study of different parameters, *Fresenius Environmental Bulletin*, 4a(2011) 1036-1045.
- [32] P. Lazar, F. Karlický, P. Jurečka, M. Kocman, E. Otyepková, K. Šafářová, et al., Adsorption of Small Organic Molecules on Graphene, *J. Am. Chem. Soc.*, 135(2013) 6372-6377.
- [33] W. Wang, Y. Zhang, Y.-B. Wang, Noncovalent  $\pi\cdots\pi$  interaction between graphene and aromatic molecule: Structure, energy, and nature, *The Journal of Chemical Physics*, 140(2014) 094302.
- [34] E. Munusamy, S.E. Wheeler, Endohedral and exohedral complexes of substituted benzenes with carbon nanotubes and graphene, *The Journal of Chemical Physics*, 139(2013) 094703.
- [35] A.L. Ringer, M.O. Sinnokrot, R.P. Lively, C.D. Sherrill, The Effect of Multiple Substituents on Sandwich and T-Shaped  $\pi$ - $\pi$  Interactions, *Chemistry – A European Journal*, 12(2006) 3821-3828.
- [36] S.E. Wheeler, K.N. Houk, Substituent Effects in the Benzene Dimer are Due to Direct Interactions of the Substituents with the Unsubstituted Benzene, *J. Am. Chem. Soc.*, 130(2008) 10854-10855.
- [37] S.L. Cockroft, J. Perkins, C. Zonta, H. Adams, S.E. Spey, C.M.R. Low, et al., Substituent effects on aromatic stacking interactions, *Organic & Biomolecular Chemistry*, 5(2007) 1062-1080.
- [38] T. Kar, H.F. Bettinger, S. Scheiner, A.K. Roy, Noncovalent  $\pi$ - $\pi$  Stacking and CH--- $\pi$  Interactions of Aromatics on the Surface of Single-Wall Carbon Nanotubes: An MP2 Study, *J. Phys. Chem. C*, 112(2008) 20070-20075.
- [39] E.C. Lee, D. Kim, P. Jurečka, P. Tarakeshwar, P. Hobza, K.S. Kim, Understanding of Assembly Phenomena by Aromatic-Aromatic Interaction: Benzene Dimer and the Substituted Systems, *J. Phys. Chem. A*, 111(2007) 3446-3457.

- [40] S.E. Wheeler, Understanding Substituent Effects in Noncovalent Interactions Involving Aromatic Rings, *Acc. Chem. Res.*, 46(2012) 1029-1038.
- [41] H. Li, Q. Zhang, N. Peng, N. Liu, Y.C. Lee, O.K. Tan, et al., Charge-Trapping Effects Caused by Ammonia in Carbon Nanotubes, *J. Nanosci. Nanotechnol.*, 7(2007) 335-338.
- [42] T. Kokabu, K. Takashima, S. Inoue, Y. Matsumura, T. Yamamoto, Transport phenomena of electrons at the carbon nanotube interface with molecular adsorption, *J. Appl. Phys.*, 122(2017) 015308.
- [43] J. Li, Y. Lu, Q. Ye, M. Cinke, J. Han, M. Meyyappan, Carbon Nanotube Sensors for Gas and Organic Vapor Detection, *Nano Lett.*, 3(2003) 929-933.
- [44] F. Tournus, S. Latil, M.I. Heggie, J.C. Charlier,  $\pi$ -stacking interaction between carbon nanotubes and organic molecules, *Phys. Rev. B*, 72(2005) 075431.
- [45] L.M. Woods, Ş.C. Bădescu, T.L. Reinecke, Adsorption of simple benzene derivatives on carbon nanotubes, *Phys. Rev. B*, 75(2007) 155415.
- [46] F. Tournus, J.C. Charlier, Ab initio study of benzene adsorption on carbon nanotubes, *Phys. Rev. B*, 71(2005) 165421.

**Figures captions:**

**Scheme 1:** Schematic presentation of the different macrocycles (MCs) (upper panel) and the potentially existing type of interactions induced by the peripheral groups (lower panel).

**Table 1:** Studied VOCs and their potential type of interactions with aromatic center or alkyl groups.

**Fig. 1:** Frequency shift measured at room temperature (25 °C) for macrocycles exposed to xylene (CuPctBu at 500 ppm , OEPH<sub>2</sub> at 450 ppm and TTPH<sub>2</sub> at 520 ppm) in dried air.

**Fig. 2:** Calibration curves of QCM coated with macrocycles as function of the benzene (2A) and xylene (2B) concentrations at room temperature (25 °C). Equations corresponding to linearization by least square method are given.

**Table 2:** Response and recovery times measured for the macrocycles exposed to BTX at room temperature (25 °C).

**Scheme 2:** Representation of the functionalization of CNTs (upper panel) and VOCs adsorption on the hybrid materials (lower panel). Sites (1) define the Naked-CNTs surface and sites (2) define the occupied CNTs surface.

**Fig. 3:** Focus on one exposure cycle of QCM response for the CNTs/OEPH<sub>2</sub> in reaction with 500 ppm benzene (A), Toluene (B) and Xylene (C). The red section represents the most rapid kinetics while the dark blue part in Fig. 3B and 3C display a slow and more persistent desorption. Experiments are performed at room temperature (25 °C).

**Table 3:** Sensor sensitivities (S) calculated from the QCM response of the CNTs/MCs in the range 33 – 500 ppm and given in  $\mu\text{Hz}/\text{ng/ppm}$ .

**Scheme 3:** Focus on the interaction of aromatic VOCs on the CNTs/MCs surfaces. Sites (1) and (2) refer to Naked-CNTs surface and MCs-occupied CNTs surface.

**Table 4:** Relative strength of the potential interactions and their influence on the kinetic of desorption

**Fig. 4:** Focus on one cycle of exposure of resistive sensor response given as  $\Delta R$  for the CNTs/CuPctBu in reaction with benzene (A), toluene (B) and xylene (C) at room temperature (25 °C). The red part of the curve represents the most rapid kinetics between 30 seconds (benzene), 1.5 minutes (toluene) and 2 minutes (xylene).

**Table 5:** Response and recovery times for the mass and resistive sensors based on the CNTs/MCs materials. NA: Not Available; because of the weak and unstable responses.

**Fig. 5:** Focus one section of dynamic QCM response of the CNTs/OEPH<sub>2</sub> sensor to benzene (A) and projection of the red frame (the sigmoid section) mathematically fitted ( $R^2=0.997$ ) with a sigmoidal function (B).

**Table 6:** Summary of the sigmoidal fitting for the CNTs/MCs giving the width (dx) and the corresponding correlation coefficient ( $R^2$ ).

**Fig. 6:** Sequential submission exposure of toluene to CNTs/OEPH<sub>2</sub> upon variation of the submission duration.

**Fig. 7:** Sensitivity of the CNTs/OEPH<sub>2</sub> materials as function of the relative humidity for BTX exposure.